CONSIDERATIONS ON THE R-CURVE OF HUMAN CORTICAL BONE

Glynn Gallaway[1]*, Matheus Dias da Rocha[1,2], Laura J. Pyrak-Nolte[1], and Thomas Siegmund[1]

[1]Purdue University, West Lafayette, IN, USA, [2]Universidade Federal do Rio de Janeiro, Rio de Janerio, Brazil
** Presenting Author email: ggallawa@purdue.edu*

Abstract
Human bone presents several factors which complicate the evaluation of fracture. Several toughening mechanisms protect humans from health complications, but also contribute to a unique 3D crack geometry. In this study, we combine 3D imaging, in-situ loading (in air and with a waterbath), and computational analysis for the interpretation of the toughness measurements of human cortical bone in the aging human population.

1. Introduction

Experimental and computational studies of fracture toughness in bone has attracted interest throughout the past. However, uncertainty still surrounds the results of these studies due to inherent challenges presented by bone. These challenges primarily arise from the hierarchical micro- and nano-structure of bone which has adapted and evolved to employ several toughening mechanisms across length scales. Studies have shown a steeply rising R-curve phenomena [1] and presented theories on cohesive zone fracture [2]. This likely occurs due to some combination of bone microstructure, matrix heterogeneity, and other non-linear behaviors. While the fracture process occurs in 3D, scientific limitations often lead to evaluations in 2D which fails to capture a full fracture process. Additionally, 2D evaluation considers plane stress, while plane strain in 3D is more physiologically relevant. Accurate fracture toughness methods are needed to characterize bone quality in treatment of bone diseases. As bone disease continues to rise in the US and around the world, development of efficient and accurate treatment methods will become vital to the maintainance of quality of life and to reduce the strain on the healthcare system. This paper describes new methods to combine in situ loading with 3D imaging, complemented by FEA simulations and SEM imaging to reduce uncertainty in fracture toughness measures.

2. Approach and Results

Unfixed human cortical bone (92Y, Male) is sectioned using a high-speed diamond blade saw (Buehler) to fabricate 4 x 4 x 24 mm^3 beams with the beam axis aligned with the long-axis of the femur. A transverse defect is assumed to exist as a result of focal osteoporsis. Beams are notched at the center to half height with a root radius of 100 μm. A sharp pre-crack is induced using a razor blade in a 1 μm diamond paste suspension. Beams are kept frozen in saline soaked gauze and defrosted overnight before testing. In-situ testing is performed with a 5000 N CT load cell (Deben) fitted into an XRADIA 510 Versa 3D X-Ray Microscope (Zeiss). Beams are arranged in either a 3- or 4-point bending configuration for standard SENB tests with a loading rate of 0.1 mm/min in a bath of phosphate buffered saline. Initially, beams are loaded to 25 N and then in 10 N increments with intermittent 3D imaging until failure is achieved. Images (with a resolution of 4.2 μm) are obtained by using 80 kV, 7W, FOV 4.2 mm, exposure 5 s, with a low energy filter. Fracture geometries are segmented using a threshold (Simpleware), and crack extension, CMOD, and kink angle are measured. Young's modulus is computed from the specimen compliance for individual beams. Preliminary experiments were performed in air, experiments in physiologic solution are on-going. Global and local stress intensity factors (for mode 1 and 2) are calculated along with J-integral components to develop an R-curve. Post fracture imaging of fracture surfaces is conducted in a SEM.

Specimens present complex fracture geometries (Fig. 1a) that indicate crack deflection, typically at weaker cement lines, osteon pullout, and osteon bridging and osteon fracture. Comparison of images across time, indicates surface crack extension is less than internal extension (Fig. 1b) and that difference reaches up to 200 μm at approximately 1,000 μm crack extension. Crack kinking angles vary along the crack front. When surface crack extension is used to construct R-curve, toughness is overestimated (Fig 1b). The fracture surface images (Fig. 2) together with the crack reconstruction (Fig. 1a) indicate that crack initiation is dominated by bone matrix fracture and that crack growth is associated with osteonal unit failure. The length

scale associated with the osteonal unit failure is of the order of 200 μm in the particular samples under investigation. Consequently, during crack growth of Δa_{max}=1,000 μm, the crack traverses only 5 of such units (Fig. 2). As a consequence of the small number of unit events during crack growth, a fracture model assuming a self-similar crack growth is insufficient to characterize the R-curve.

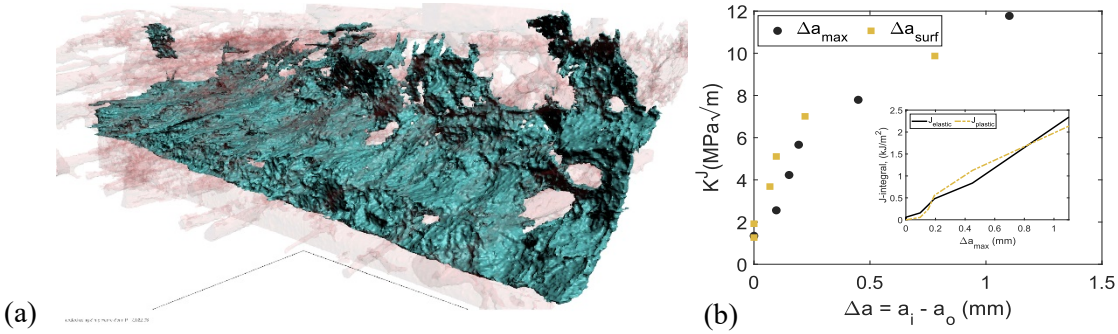

Figure 1: (a) 3D reconstruction of fracture (beige) with haversian canal structure (transparent red), (b) Effective toughness vs maximum internal and surface crack length with inset for an R-curve with J.

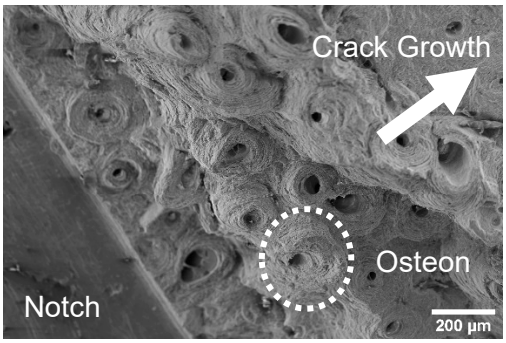

Figure 2: Fracture surface of cortical bone specimen. The unit fracture event is that of an osteonal unit.

3. Discussion and Conclusions

In Yang et al. [2] and Kim at al. [3], cortical bone longitudinal/splitting failure was analyzed within the framework of cohesive zone models. While the present data on R-curves for transverse loading conditions related well with those of Koester et al. [1], the cohesive zone model analysis approach of [2, 3] has not been applied in such conditions. Our analysis extends the approach of [2, 3, 4] to the transverse bone fracture problem. We thereby employ a cohesive zone law describing matrix failure as processes characterized by high strength and short material separation length, combined with a representation of osteonal failure with low strength and large material separation length. Then, the R-curve is the outcome of an analysis in which crack initiation toughness represents the cohesive energy of matrix fracture and the rising R-curve that of the build-up of dissipation due to the osteonal unit failure processes.

Reference

[1] Koester, K.J., Ager, J.W. and Ritchie, R.O., 2008. *Nature materials*, *7*(8), pp.672-677. **[2]** Cox, B. and Yang, Q., *Eng. Fract. Mech.* (2007). **[3]** Kim, KT., Bažant, Z.P., and Yu, Q., *Int. J. Fract.* (2013). **[4]** Han, J. and Siegmund, T., *J. Adhes. Sci. Technol.* (2012).

Acknowledgements

This work is finacially supported by NSF award 1952993; G.G. supported by NSF GRF number DGE-1842166.